JOURNAL OF GUIDANCE, CONTROL, AND DYNAMICS
Vol. 15, No. 5, September–October 1992

Loop Transfer Recovery Approach to H_∞ Design for the Coupled Mass Benchmark Problem

Edward V. Byrns Jr.*
Systems Planning and Analysis, Inc., Falls Church, Virginia 22041
and
Anthony J. Calise†
Georgia Institute of Technology, Atlanta, Georgia 30332

This paper presents fixed-order dynamic compensator designs for the coupled mass benchmark problem. The design technique uses a method for loop transfer recovery at the plant input to approximately recover the transfer properties of an H_∞ controller with full state feedback. The recovery is accomplished by the unique selection of quadratic performance index weighting matrices in a standard optimal output feedback formulation for fixed-order compensation. For the benchmark control problem, two compensator designs are developed. These designs use an observer canonical form to represent the compensator dynamics. The first design addresses problem 1, where only the spring stiffness is uncertain. The second design, a solution to problem 3, provides asymptotic rejection of a sinusoidal disturbance in the presence of an uncertain spring stiffness.

Introduction

THE coupled mass benchmark problem[1] has been addressed using a variety of controller design techniques. Both classical and modern approaches have been applied to this problem, which involves two masses that are interconnected by a single spring, as shown in Fig. 1. It is simple to formulate, but contains many characteristics that from a control viewpoint are typical of large flexible structures with noncollocated sensors and actuators. The design objectives include disturbance rejection and robust stability and performance in the presence of plant parameter variations.

In Refs. 2–4, a technique is developed to design H_∞ controllers that have reduced parameter sensitivity. This approach uses internal feedback loop (IFL) modeling to represent the uncertain system. The advantage of this technique is that it is easily incorporated into a state-space formulation. In Refs. 2 and 3, several H_∞ output feedback controllers are designed for the coupled mass benchmark problem. In Ref. 4, this technique is used to design two reduced sensitivity H_∞ full state feedback controllers for the Space Station.

One disadvantage of H_∞ output feedback design techniques is that the order of the resulting controller may be extremely large, once the frequency weighting filters are introduced at the plant input and output. In Ref. 5, a method for loop transfer recovery (LTR) at the plant input is developed for designing fixed-order dynamic compensators that approximately recover the loop properties of an H_∞ controller with full state feedback. This design technique requires two steps. First, a full state feedback H_∞ controller is designed to satisfy the design objectives. Second, by a unique selection of the quadratic performance index weighting matrices, a fixed-order dynamic compensator is designed to approximately recover the properties of the full state controller. By using an observer canonical form[6] to parameterize the compensator, the design can be reformulated as a constant gain output feedback problem.

In this paper, the reduced parameter sensitivity H_∞ design technique is combined with the approximate LTR compensator design methodology to provide robust fixed-order dynamic compensators that have reduced sensitivity to uncertain parameters. Specifically, the reduced parameter sensitivity formulation is used to design the full state H_∞ controller. The dynamic compensator is then designed to approximately recover the performance and robustness of the full state controller. This technique is illustrated by three compensator designs for the coupled mass benchmark problem.

This paper is organized as follows. First, the reduced parameter sensitivity full state H_∞ design technique is presented. This section contains a review of both the IFL modeling and the full state H_∞ controller design. Next, the observer canonical form and approximate LTR compensator design methodology is given. Finally, the paper concludes with three design examples for the coupled mass benchmark problem. The first design addresses problem 1, where only the spring stiffness is uncertain. This design is compared with the results presented in Ref. 2. The second design, a solution to problem 3, provides asymptotic rejection of a sinusoidal disturbance in the presence of an uncertain spring stiffness.

Reduced Parameter Sensitivity H_∞ Full State Controller

The IFL modeling technique, originally developed in Ref. 7, is a method that transforms an uncertain system into a convenient input/output decomposition. This decomposition produces fictitious inputs and outputs that are related by an internal feedback loop gain matrix. When the fictitious inputs and outputs are combined with the nominal system, a two-input/two-output (TITO) system results, which can then be incorporated into a standard H_∞ design methodology. In this section, the IFL approach to H_∞ design[2–4] is outlined for the case of full state feedback.

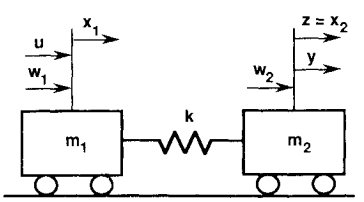

Fig. 1 Coupled mass benchmark problem.

Received April 24, 1991; revision received Dec. 11, 1991; accepted for publication Dec. 18, 1991.

*Analyst. Member AIAA.

†Professor, School of Aerospace Engineering. Associate Fellow AIAA.

Internal Feedback Loop Modeling

Consider the linear system

$$\begin{Bmatrix} \dot{x} \\ z \end{Bmatrix} = \begin{bmatrix} \hat{A} & \hat{B}_1 & \hat{B}_2 \\ C_1 & 0 & D_{12} \end{bmatrix} \begin{Bmatrix} x \\ w \\ u \end{Bmatrix} \qquad \begin{matrix} x \in \mathcal{R}^n & w \in \mathcal{R}^{m_1} & u \in \mathcal{R}^{m_2} \\ z \in \mathcal{R}^{p_1} & y \in \mathcal{R}^{p_2} \end{matrix} \tag{1}$$

where w is a disturbance input, u the control input, and z the controlled output vector. The matrices $\hat{A}$, $\hat{B}_1$, and $\hat{B}_2$ are subject to parameter variations, whereas C_1 and D_{12} are not. The system in Eq. (1) can be decomposed as

$$\begin{Bmatrix} \dot{x} \\ z \end{Bmatrix} = \left\{ \begin{bmatrix} A & B_1 & B_2 \\ C_1 & 0 & D_{12} \end{bmatrix} + \Delta_p \right\} \begin{Bmatrix} x \\ w \\ u \end{Bmatrix} \tag{2}$$

where A, B_1, and B_2 represent the nominal plant parameter matrices, and Δ_p is the perturbation matrix given by

$$\Delta_p = \begin{bmatrix} \Delta A & \Delta B_1 & \Delta B_2 \\ 0 & 0 & 0 \end{bmatrix} \tag{3}$$

Assuming that ΔA, ΔB_1, and ΔB_2 are affine functions of s independent parameters, $p_1, \ldots, p_s$, then the perturbation matrix can be expressed by the following nonunique decomposition:

$$\Delta_p = -\begin{bmatrix} M_x \\ 0 \end{bmatrix} E[N_x \quad N_w \quad N_u] = -MEN \tag{4}$$

where

$$E = \text{diag}\{\Delta p_1, \ldots, \Delta p_s\}, \qquad |\Delta p_i| \leq 1 \tag{5}$$

Note that M and N can always be scaled such that $|\Delta p_i| \leq 1$. Using the IFL approach, a fictitious output is defined as

$$z_f = [N_x \quad 0 \quad N_w \quad N_u] \begin{Bmatrix} x \\ w_f \\ w \\ u \end{Bmatrix} \tag{6}$$

where w_f is a fictitious input, and E is the fictitious internal feedback loop gain. Combining Eqs. (4) and (6) with the nominal system, the TITO system is then given by

$$\begin{Bmatrix} \dot{x} \\ z_f \\ z \end{Bmatrix} = \begin{bmatrix} A & M_x & B_1 & B_2 \\ N_x & 0 & N_w & N_u \\ C_1 & 0 & 0 & D_{12} \end{bmatrix} \begin{Bmatrix} x \\ w_f \\ w \\ u \end{Bmatrix} \tag{7}$$

$$w_f = -Ez_f \tag{8}$$

By defining the following variables

$$\bar{z} = \begin{Bmatrix} z_f \\ z \end{Bmatrix}, \qquad \bar{w} = \begin{Bmatrix} w_f \\ w \end{Bmatrix} \tag{9}$$

$$\bar{B}_1 = [M_x \quad B_1], \qquad \bar{C}_1 = \begin{bmatrix} N_x \\ C_1 \end{bmatrix} \tag{10}$$

$$\bar{D}_{11} = \begin{bmatrix} 0 & N_w \\ 0 & 0 \end{bmatrix}, \qquad \bar{D}_{12} = \begin{bmatrix} N_u \\ D_{12} \end{bmatrix} \tag{11}$$

then Eq. (7) can be rewritten as

$$\begin{Bmatrix} \dot{x} \\ \bar{z} \end{Bmatrix} = \begin{bmatrix} A & \bar{B}_1 & B_2 \\ \bar{C}_1 & \bar{D}_{11} & \bar{D}_{12} \end{bmatrix} \begin{Bmatrix} x \\ \bar{w} \\ u \end{Bmatrix} \tag{12}$$

which has a similar structure as Eq. (1). Using Eq. (12), an H_∞ full state feedback controller can be computed that has a guaranteed stability boundary and a robust performance property.

Full State H_∞ Controller

A state-space solution for the full state H_∞ feedback control problem is given in Ref. 8. The main result can be summarized as follows. Given a system of the form in Eq. (12), assume that 1) $(A, \bar{B}_1)$ is stabilizable and $(\bar{C}_1, A)$ is detectable; 2) (A, B_2) is stabilizable; 3) $\bar{D}_{12}^T[\bar{C}_1 \quad \bar{D}_{12}] = [0 \quad I]$; and 4) $\bar{D}_{11} = 0$. Then it can be shown that there exists an internally stabilizing controller such that the closed-loop transfer function from disturbance inputs to controlled outputs $T_{\bar{z}\bar{w}}$ satisfies

$$\|T_{\bar{z}\bar{w}}\|_\infty < \gamma \tag{13}$$

if and only if $H \in \text{domain}\{\text{Ric}\}$ and $X = \text{Ric}\{H\} \geq 0$, where

$$H = \begin{bmatrix} A & \frac{1}{\gamma}\bar{B}_1\bar{B}_1^T - B_2B_2^T \\ -\bar{C}_1^T\bar{C}_1 & -A^T \end{bmatrix} \tag{14}$$

One such full state controller is given by

$$u = -K_\infty x, \qquad K_\infty = B_2^T X \tag{15}$$

Note that assumption 4 imposes the restriction that $N_w = 0$, which implies that there is no uncertainty in B_1. However, in general, real parameter uncertainty in B_1 may affect performance but not stability. Therefore, it follows that the system in Eq. (1) with $u = -K_\infty x$ is stable for all $|\Delta p_i| \leq 1/\gamma$ and that for $\Delta B_1 = 0$, $\|z\|_2 < \gamma$ for all $w(t)$ such that $\|w\|_2 \leq 1$.

Approximate Recovery of H_∞ Loop Shapes

In Ref. 5, an approximate LTR method is presented for recovery of closed-loop transfer function properties from disturbance inputs to controlled outputs. This formulation is based on a performance index that penalizes the difference between two closed-loop return signals, corresponding to v_1 and v_2 shown in Fig. 2. These signals are produced by uniformly distributed impulses injected at both w and w_d for zero initial conditions. The details of this procedure are reviewed in the following.

The state-space realization of the transfer function $G_{22}(s)$ from u to y is given by

$$\dot{x} = Ax + B_2u \tag{16}$$

$$y = C_2x + D_{22}u \tag{17}$$

A compensator in observer canonical form[6] for the system in Eqs. (16) and (17) can be described as

$$\dot{z}_{ob} = P_{ob}^o z_{ob} + u_{ob}, \qquad z_{ob} \in \mathcal{R}^{nc} \tag{18}$$

$$u_{ob} = P_{ob}u - Ny, \qquad u_{ob} \in \mathcal{R}^{nc} \tag{19}$$

$$u = -H^o z_{ob} \tag{20}$$

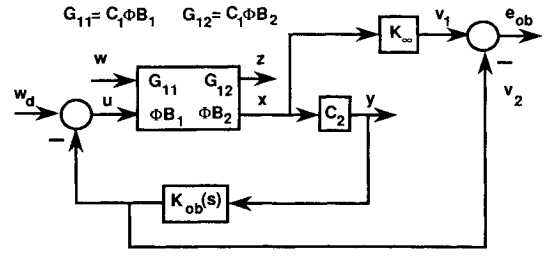

Fig. 2 Formulation to approximately recover T_{zw}.

where P_{ob} and N are free parameter matrices of compatible dimensions. The matrices P^o_{ob} and H^o are predetermined by the choice of observability indices v_i, and their structure is given in the following:

$$P^o_{ob} = \text{Block diag}[P^o_1, \ldots, P^o_{m_2}] \tag{21}$$

$$P^o_i = \begin{bmatrix} 0 & 0 & & 0 & 0 \\ 1 & 0 & \cdots & 0 & 0 \\ 0 & 1 & & 0 & 0 \\ & & \vdots & & \\ 0 & 0 & & 0 & 0 \\ & & \cdots & & \\ 0 & 0 & & 1 & 0 \end{bmatrix}_{v_i x v_i} \tag{22}$$

$$H^o = \text{Block diag}\{[0, \ldots, 0\ 1]_{1 x v_i},\ i = 1, \ldots, m_2\} \tag{23}$$

The observability indices to be chosen are subject to the following constraints:

$$\sum_{i=1}^{m_2} v_i = nc \tag{24}$$

$$v_i \leq v_{i+1} \tag{25}$$

The compensator transfer function is given by

$$K_{ob}(s) = H^o(sI - \boldsymbol{P}_{ob})^{-1}N \tag{26}$$

where

$$\boldsymbol{P}_{ob} = P^o_{ob} - P_{ob}H^o \tag{27}$$

This compensator form permits a compact formulation for the following constant gain output feedback problem. The system in Eqs. (16) and (17) is augmented with the observer canonical compensator, Eqs. (18–20), which results in

$$\dot{\boldsymbol{x}} = \boldsymbol{A}\boldsymbol{x} + \boldsymbol{B}u_{ob}, \qquad \boldsymbol{x} \in \mathcal{R}^{n+nc} \tag{28}$$

$$\boldsymbol{y} = \boldsymbol{C}\boldsymbol{x}, \qquad \boldsymbol{y} \in \mathcal{R}^{m_2+p_2} \tag{29}$$

$$u_{ob} = -\boldsymbol{G}\boldsymbol{y} \tag{30}$$

where $\boldsymbol{x}^T = \{x^T, z^T_{ob}\}$, $\boldsymbol{y}^T = \{y^T, -u^T\}$ and

$$\boldsymbol{A} = \begin{bmatrix} A & -B_2H^o \\ 0 & P^o_{ob} \end{bmatrix}, \qquad \boldsymbol{B} = \begin{bmatrix} 0 \\ I_{nc} \end{bmatrix} \tag{31}$$

$$\boldsymbol{C} = \begin{bmatrix} C_2 & 0 \\ 0 & H^o \end{bmatrix}, \qquad \boldsymbol{G} = [N \quad P_{ob}] \tag{32}$$

Note that the free parameter matrices used in designing the compensator are compactly placed in the equivalent constant gain feedback matrix $\boldsymbol{G}$. The error signal to be penalized is given by

$$e_{ob} = v_1 - v_2 = K_x x - H^o z_{ob} \tag{33}$$

where the full state gain K_x is a full state H_∞ controller designed to meet robust stability and performance specifications.

The approximate LTR performance index is

$$J = E_{x_o}\left\{\int_o^\infty [e^T_{ob}e_{ob} + \rho u^T_{ob}u_{ob}]\, dt\right\} \tag{34}$$

Substituting of Eq. (33) into Eq. (34), and rewriting the performance index as

$$J = E_{x_o}\left\{\int_o^\infty [\boldsymbol{x}^T\boldsymbol{Q}\boldsymbol{x} + u^T_{ob}Ru_{ob}]\, dt\right\} \tag{35}$$

yields the following plant and compensator state weighting matrices:

$$Q = \begin{bmatrix} K^T_x K_x & -K^T_x H^o \\ -H^{oT}K_x & H^{oT}H^o \end{bmatrix}, \qquad R = \rho I_{nc} \tag{36}$$

By injecting uniformly distributed impulses at both the control and disturbance inputs, the following initial condition variance is produced:

$$E\{\boldsymbol{x}_o\boldsymbol{x}^T_o\} = \boldsymbol{x}_o = \begin{bmatrix} \overline{B}\,\overline{B}^T & 0 \\ 0 & 0 \end{bmatrix}; \qquad \overline{B} = [\overline{B}_1 \quad B_2]W \tag{37}$$

where W is used to individually weight the impulse strengths produced by $\overline{B}$. It is required that $\overline{B}$ span the column space of $[\overline{B}_1 \quad B_2]$.

Equations (28–30) and (35) constitute a constant gain output feedback problem whose necessary conditions for optimality are well known.[9] As the parameter $\rho \to 0$, then $T_{\overline{z}\overline{w}}$ of the compensator approximates $T_{\overline{z}\overline{w}}$ of the full state H_∞ controller to varying degrees depending on the order of the compensator.

Coupled Mass Benchmark Problem Controller Design

This design problem involves two masses that are interconnected by a single spring; see Fig. 1. The system dynamics are given by

$$\dot{x} = \begin{bmatrix} 0 & 0 & 1 & 0 \\ 0 & 0 & 0 & 1 \\ -k/m_1 & k/m_1 & 0 & 0 \\ k/m_2 & -k/m_2 & 0 & 0 \end{bmatrix} x + \begin{bmatrix} 0 \\ 0 \\ 1/m_1 \\ 0 \end{bmatrix} u + \begin{bmatrix} 0 & 0 \\ 0 & 0 \\ 1/\overline{m}_1 & 0 \\ 0 & 1/\overline{m}_2 \end{bmatrix} \begin{Bmatrix} w_1 \\ w_2 \end{Bmatrix} \tag{38}$$

$$y = [0 \quad 1 \quad 0 \quad 0]x \tag{39}$$

where $x = \{x_1, x_2, \dot{x}_1, \dot{x}_2\}^T$ and the nominal parameter values for m_1, m_2, and k are $\overline{m}_1 = \overline{m}_2 = \overline{k} = 1.0$. The natural frequency is at $\omega_n = 1.4$ rad/s. Observe that the control input acts on mass 1, whereas only the displacement of mass 2 is sensed. In addition, note that for modeling purposes the disturbance input matrix depends only on the nominal values of m_1 and m_2. This restriction ensures that $\overline{D}_{11} = 0$ in the reduced parameter sensitivity H_∞ design formulation.

Problem 1

For this design, the nominal performance specification calls for a 90% settling time of 15 s on the mass 2 displacement, when a unit impulse is injected at w_2. There is also a robust stability specification that the closed-loop system remain stable for the range of spring stiffness, $0.5 \leq k \leq 2.0$. Beyond this, the controller complexity, the control effort, performance robustness, bandwidth, and response to measurement noise should all be reasonable.

Problem 2

Same as problem 1, except that the stability and performance should be maintained in the presence of three uncertain parameters: k, m_1, and m_2. This problem is not addressed in this paper.

Problem 3

Same as problem 1, except that for this problem w_2 is a sinusoidal disturbance of frequency 0.5 rad/s, with unknown but constant amplitude and phase. The objective of this design is to obtain asymptotic rejection of this disturbance in the

mass 2 displacement, with a settling time of 20 s. The controller must remain stable for $\bar{m}_1 = \bar{m}_2 = 1.0$ and $0.5 \leq k \leq 2.0$.

For each design problem, the H_∞ full state controller design closely parallels the H_∞ output feedback designs in Ref. 2.

Problem 1 Results

For the design with an uncertain spring stiffness of the form $k = \bar{k} + \Delta k$, the perturbation matrix Δ_p is given by

$$\Delta_p = \begin{bmatrix} \Delta A & 0 & 0 \\ 0 & 0 & 0 \end{bmatrix} \tag{40a}$$

where

$$\Delta A = \begin{bmatrix} 0 & 0 & 0 & 0 \\ 0 & 0 & 0 & 0 \\ -\Delta k & \Delta k & 0 & 0 \\ \Delta k & -\Delta k & 0 & 0 \end{bmatrix} \tag{40b}$$

which can be decomposed as in Eq. (4) by selecting

$$M_x = [0 \quad 0 \quad 1 \quad -1]^T, \qquad N_x = [1 \quad -1 \quad 0 \quad 0]$$

$$N_w = N_u = 0 \tag{41}$$

Selecting the performance variable as $z = \{x_2, u\}^T$, then

$$\bar{B}_1 = \begin{bmatrix} 0 & 0 & 0 \\ 0 & 0 & 0 \\ 1 & 1 & 0 \\ -1 & 0 & 1 \end{bmatrix}, \qquad \bar{C}_1 = \begin{bmatrix} 1 & -1 & 0 & 0 \\ 0 & 1 & 0 & 0 \\ 0 & 0 & 0 & 0 \end{bmatrix}$$

$$\bar{D}_{12} = \begin{bmatrix} 0 \\ 0 \\ 1 \end{bmatrix} \tag{42}$$

In this example, the disturbances w_f, w_1, and w_2 are multiplied by weighting factors of 0.1, 0.025 and 0.025, respectively. These weighting factors represent the relative disturbance level. For $\gamma = 1$, the full state suboptimal H_∞ feedback gain is given by

$$K_\infty = [1.509 \quad -0.496 \quad 1.740 \quad 0.935] \tag{43}$$

A third-order compensator is selected to recover the loop properties of the H_∞ full state controller. The constant gain output feedback problem is solved using a convergent sequential numerical algorithm[10] and the resulting compensator with $\rho = 1.0E\text{-}6$ in Eqs. (36) and $\bar{B} = \bar{B}_1$ in Eq. (37) is given in the following:

$$\dot{z}_{ob} = \begin{bmatrix} 0 & 0 & -5.073 \\ 1 & 0 & -6.093 \\ 0 & 1 & -3.240 \end{bmatrix} z_{ob} + \begin{bmatrix} 0.509 \\ 2.799 \\ -2.820 \end{bmatrix} y$$

$$u = -[0 \quad 0 \quad 1] z_{ob} \tag{44}$$

The approximate recovery of $T_{\bar{z}\bar{w}}$ is shown in Fig. 3 by comparing the maximum singular values of $T_{\bar{z}\bar{w}}$ with full state feedback to those obtained for two compensator designs. Note that as ρ is reduced, $\|T_{\bar{z}\bar{w}}\|_\infty$ is reduced while sacrificing recovery at the low-frequency end. When $\rho = 1.0E\text{-}6$, $\|T_{\bar{z}\bar{w}}\|_\infty \approx -10$ dB, which is a significant reduction from $\|T_{\bar{z}\bar{w}}\|_\infty \approx -1$ dB for $\rho = 1.0$.

Figure 4 shows the sensitivity root locus of the closed-loop system as k is varied. This design remains stable for the range $0.50 \leq k \leq 4.08$. Figure 5 shows the system response to a unit impulse at w_2. Note that the 90% settling time is approximately 15 s and that the peak x_2 displacement is near 1.8. The control effort appears to be reasonable.

Figure 6 shows the frequency response plots for the dynamic compensator transfer function. This controller is nonminimum phase, and it stabilizes the system by providing phase lag at the flexible mode natural frequency.

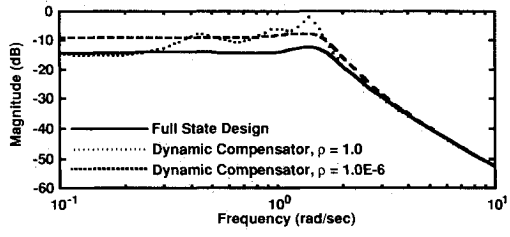

Fig. 3 Approximate recovery of $T_{\bar{z}\bar{w}}$ for problem 1.

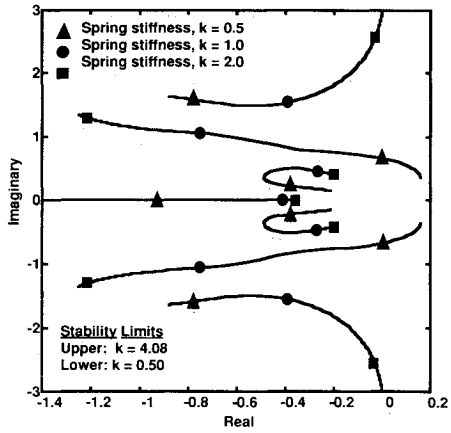

Fig. 4 Root locus vs spring stiffness for problem 1.

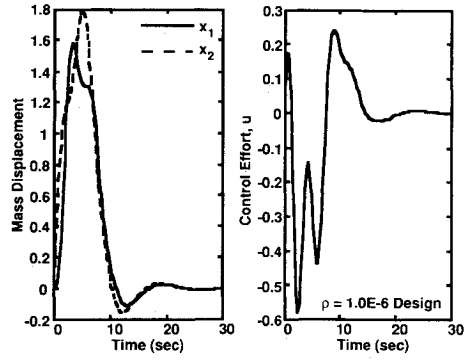

Fig. 5 System response for unit impulse at w_2.

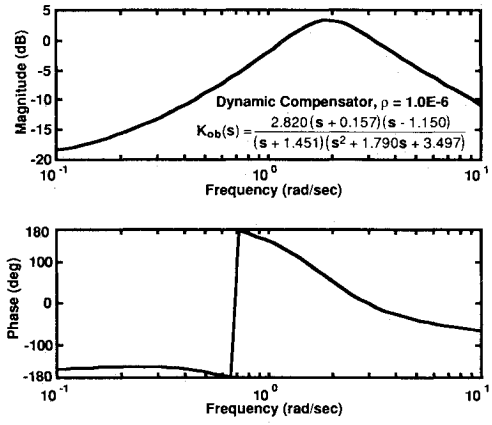

Fig. 6 Dynamic compensator transfer function for problem 1.

Next, a full-order dynamic compensator is designed using the approximate LTR procedure. For $\rho = 1.0E\text{-}6$, the compensator is given by

$$\dot{z}_{ob} = \begin{bmatrix} 0 & 0 & 0 & -56.80 \\ 1 & 0 & 0 & -55.84 \\ 0 & 1 & 0 & -30.92 \\ 0 & 0 & 1 & -5.579 \end{bmatrix} z_{ob} + \begin{bmatrix} 5.987 \\ 29.85 \\ -33.17 \\ 6.573 \end{bmatrix} y$$

$$u = -[0 \quad 0 \quad 0 \quad 1] z_{ob} \tag{45}$$

The maximum singular values of $T_{\bar{z}\bar{w}}$ for this design are compared with $T_{\bar{z}\bar{w}}$ for the full state design in Fig. 7. A comparison of Figs. 3 and 7 shows that the third-order compensator design achieves nearly the same degree of recovery as the full-order compensator. For the full-order compensator, further recovery (i.e., smaller values of ρ) results in extremely large gains. It can be shown that the standard LTR procedure[13] also exhibits this behavior. Complete recovery of the appropriate loop shapes is possible only with excessively high-frequency compensator modes.

The dynamic compensators in Eqs. (44) and (45) are very similar to three previously published designs. In Ref. 2, a full-order output feedback H_∞ controller was designed using the IFL technique. In Ref. 11, the controller is a fixed-order dynamic compensator in controller canonical form, which was designed by an approximate LTR method to achieve sensitivity reduction while maintaining performance at the plant output. Lastly, in Ref. 12, the controller is a nonminimum phase all-pass structural filter designed using classical techniques. In Table 1, the performance of these three designs are compared to the compensator in Eqs. (44). Note that all of these design techniques result in a nonminimum phase compensator, with the nonminimum phase zero near the system natural frequency. In essence, robustness is achieved by improving the phase margin.

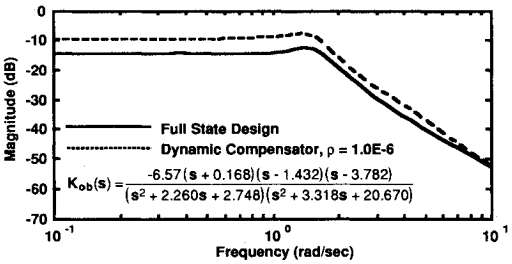

Fig. 7 Approximate recovery of $T_{\bar{z}\bar{w}}$ for problem 1 using a full-order compensator.

Problem 3 Results

For this design, the disturbance at w_2 is given by

$$w_2 = \sin(0.5t) \tag{46}$$

To achieve asymptotic rejection of w_2, a disturbance rejection filter is defined as

$$\ddot{\alpha} + (0.5)^2\alpha = x_2 \tag{47}$$

and the plant dynamics are augmented with the filter dynamics by defining

$$A = \begin{bmatrix} 0 & 0 & 1 & 0 & 0 & 0 \\ 0 & 0 & 0 & 1 & 0 & 0 \\ -k & k & 0 & 0 & 0 & 0 \\ -k & k & 0 & 0 & 0 & 0 \\ 0 & 0 & 0 & 0 & 0 & 1 \\ 0 & 1 & 0 & 0 & -0.25 & 0 \end{bmatrix},$$

$$B_1 = \begin{bmatrix} 0 & 0 \\ 0 & 0 \\ 1 & 0 \\ 0 & 1 \\ 0 & 0 \\ 0 & 0 \end{bmatrix}, \quad B_2 = \begin{bmatrix} 0 \\ 0 \\ 1 \\ 0 \\ 0 \\ 0 \end{bmatrix} \tag{48}$$

where $x = \{x_1, x_2, \dot{x}_1, \dot{x}_2, \alpha, \dot{\alpha}\}^T$. The outputs of the augmented system are defined to be $y = \{x_2, \alpha, \dot{\alpha}\}^T$. Since x_2 drives the undamped filter in Eq. (47), asymptotic rejection of the disturbance w_2 must occur in x_2 if the closed-loop system is asymptotically stable.

To account for the uncertain spring stiffness, which is of the form $k = \bar{k} + \Delta k$, the perturbation matrix is given by

$$\Delta_p = \begin{bmatrix} \Delta A & 0 & 0 \\ 0 & 0 & 0 \end{bmatrix} \tag{49a}$$

Table 1 Comparison of controllers for problem 1

	Observer form canonical compensator	Full-order observer form canonical compensator	Full-order H_∞ output feedback controller	Controller form canonical compensator	Structural filter
Controller order	3	4	4	3	2
Gain margin, dB	2.9	3.1	3.3	4.4	2.8
Phase margin, deg	22	28	24	30	25
90% settling time, s	15	15	15	22	15
Stability range for stiffness variations	$0.5 \le k \le 4.08$	$0.51 \le k \le 3.56$	$0.44 \le k \le 3.27$	$0.55 \le k \le 5.0$	$0.70 \le k \le 2.3$

Observer canonical form compensator

$$K_{ob}(s) = \frac{2.820(s + 0.157)(s - 1.150)}{(s + 1.451)(s^2 + 1.790s + 3.497)}$$

Full-order observer canonical form compensator

$$K_{ob}(s) = \frac{-6.57(s + 0.168)(s - 1.432)(s - 3.782)}{(s^2 + 2.2600s + 2.748)(s^2 + 3.318s + 20.670)}$$

Full-order H_∞ output feedback[2]

$$K_\infty(s) = \frac{2.130(s + 0.145)(s - 0.984)(s + 3.434)}{(s^2 + 2.617s + 2.515)(s^2 + 2.0567s + 5.856)}$$

Controller canonical form compensator[11]

$$K_{co}(s) = \frac{0.1076(s + 0.20)(s - 1.3)}{(s + 73.7)(s^2 + 1.18s + 1.392)}$$

Structural filter[12]

$$K_{sf}(s) = \frac{1.67(s + 0.20)(s^2 - 1.4s + 1.96)}{(s + 2.0)(s^2 + 1.4s + 1.96)}$$

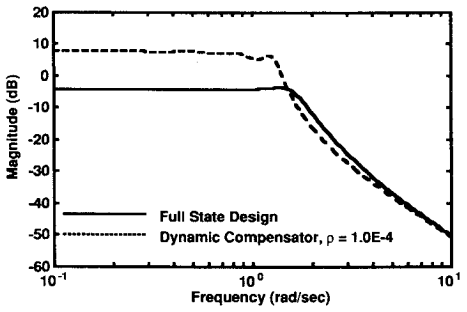

Fig. 8 Approximate recovery of $T_{\bar{z}\bar{w}}$ for problem 3.

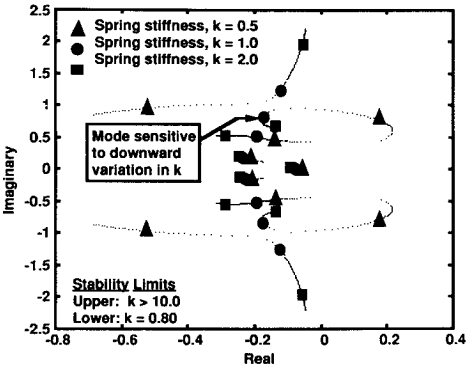

Fig. 9 Root locus vs spring stiffness for problem 3.

where

$$\Delta A = \begin{bmatrix} 0 & 0 & 0 & 0 & 0 & 0 \\ 0 & 0 & 0 & 0 & 0 & 0 \\ -\Delta k & \Delta k & 0 & 0 & 0 & 0 \\ \Delta k & -\Delta k & 0 & 0 & 0 & 0 \\ 0 & 0 & 0 & 0 & 0 & 0 \\ 0 & 0 & 0 & 0 & 0 & 0 \end{bmatrix} \tag{49b}$$

which can be decomposed as

$$M_x = [0 \quad 0 \quad 1 \quad -1 \quad 0 \quad 0]^T, \; N_x = [1 \quad -1 \quad 0 \quad 0 \quad 0 \quad 0]$$

$$N_w = N_u = 0 \tag{50}$$

The performance variables are $z = \{x_2 + 0.5\alpha + 2.0\dot{\alpha}, u\}^T$, and the disturbances w_f, w_1, and w_2 are scaled by 0.123, 0.05, 0.05, respectively. For $\gamma = 10$, the full state controller is

$$K_z = [4.250 \quad 1.597 \quad 2.916 \quad 4.931 \quad -0.710 \quad 1.732] \tag{51}$$

A third-order compensator is selected to recover the loop properties of $T_{\bar{z}\bar{w}}$. The recovery is shown in Fig. 8 for the $\rho = 1.0E\text{-}4$ design. For this design, $\bar{B} = \bar{B}_1$ in Eq. (37). Note that it is difficult to recover the low-frequency end of $T_{\bar{z}\bar{w}}$, where $\|T_{\bar{z}\bar{w}}\|_\infty \approx 9$ dB.

Figure 9 shows the sensitivity root locus of the closed-loop system to variations in spring stiffness. In the downward direction, the system remains stable until $k = 0.80$. When compared to the problem 1 design, this compensator has increased sensitivity to downward variations in spring stiffness, which is due primarily to the disturbance rejection filter mode. As k is reduced, this mode quickly becomes unstable. In the upward direction, the system remains stable for $k > 10.0$, which exceeds the upper limit for problem 1.

In Fig. 10, the time responses are shown, where the disturbance w_2 is given by Eq. (46). Note that the performance variable x_2 has a 90% settling time of less than 15 s and a peak displacement of 3.6. In steady state, x_1 oscillates at an amplitude of approximately 1.0. This motion cancels the effect of the disturbance. Again, the control effort is reasonable.

The dynamic compensator for the $\rho = 1.0E\text{-}4$ design is given by

$$\dot{z}_{ob} = \begin{bmatrix} 0 & 0 & -0.964 \\ 1 & 0 & -1.315 \\ 0 & 1 & -1.514 \end{bmatrix} z_{ob} + \begin{bmatrix} 0.055 & -0.012 & 0.028 \\ 0.395 & -0.084 & 0.040 \\ 1.045 & -0.139 & -0.108 \end{bmatrix} y$$

$$u = -[0 \quad 0 \quad 1] z_{ob} \tag{52}$$

or in transfer function form

$$K_{ob}(s) = \begin{bmatrix} \dfrac{-1.045(s^2 + 0.376s + 0.529)}{(s + 0.0804)(s^2 + 1.434s + 1.199)} \\ \dfrac{0.139(s + 0.382)(s + 0.221)}{(s + 0.0804)(s^2 + 1.434s + 1.199)} \\ \dfrac{0.108(s + 0.353)(s - 0.727)}{(s + 0.0804)(s^2 + 1.434s + 1.199)} \end{bmatrix}^T \tag{53}$$

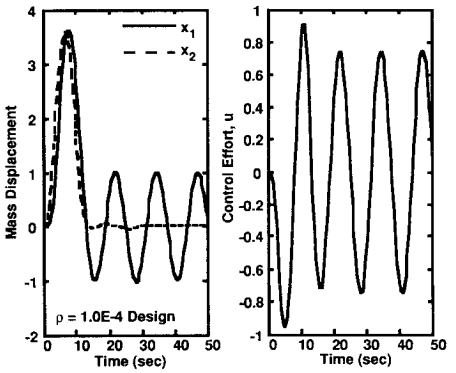

Fig. 10 System response for sinusoidal disturbance at w_2.

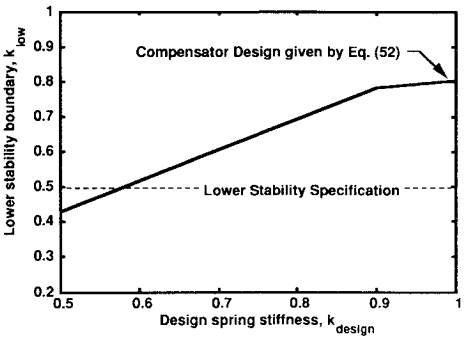

Fig. 11 Lower spring stiffness stability boundary vs design spring stiffness.

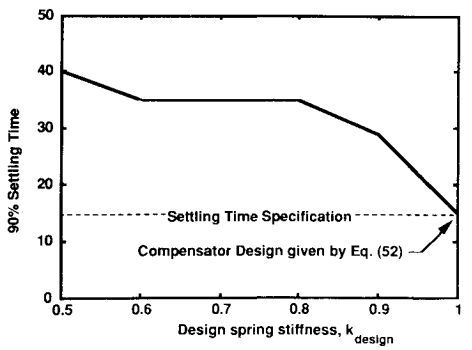

Fig. 12 90% settling time vs design spring stiffness.

Note that the (1, 3) element of $K_{ob}(s)$ has a nonminimum phase zero. For the compensators given by Eqs. (44), (45), and (64), it appears that the nonminimum phase zero is critical to stabilizing the coupled mass system.

In an effort to decrease the sensitivity to downward variations in spring stiffness, several additional compensator designs were performed. Note that γ and all weighting matrices used in the design of the compensator in Eqs. (52) are held constant in these subsequent designs. For design purposes, the nominal spring stiffness is set increasingly closer to the desired stability limit of $k = 0.5$. However, the performance and stability evaluations are conducted with a nominal spring stiffness of $\bar{k} = 1.0$. In Fig. 11, the lower stability limit k_{low} is shown as a function of the nominal design spring stiffness k_{design}. As Fig. 11 demonstrates, the lower stability boundary improves as the design spring stiffness is reduced. In fact, the lower stability specification is satisfied when $k_{\text{design}} \approx 0.6$. Note that for all of these compensator designs, the closed-loop systems remains stable for $k > 10.0$.

The improvement in robust stability is not achieved without a price. For the designs represented by Fig. 11, nominal performance is sacrificed as robust stability is improved. Figure 12 shows the 90% settling time as a function of the design spring stiffness. As k_{design} is reduced, the settling time is significantly increased. In addition, a low-amplitude "ringing" was observed to develop in the time response of the x_2 mass as k_{design} is reduced. Thus, for this problem, robust stability and nominal performance must be reasonably balanced. It is felt that the compensator in Eqs. (52) produces an acceptable solution to this problem.

Conclusions

This paper has presented three fixed-order dynamic compensators for the coupled mass benchmark problem that have reduced sensitivity to parameter variations. The compensators are designed to approximately recover the transfer function properties from disturbances to controlled outputs of a full state H_∞ controller. Robustness to a parameter uncertainty is achieved in the full state design by using an internal feedback loop modeling technique.

For each design, the fixed-order dynamic compensator is a nonminimum phase controller and is similar to previous controllers designed using both classical and modern techniques. The fixed-order dynamic compensator stabilizes the system by providing additional phase lead at the system natural frequency. In each design, the compensators provide varying degree of robust stability and performance.

References

[1]Wie, B., and Bernstein, D. S., "A Benchmark Problem for Robust Control Design," *Proceedings of the American Control Conference*, San Diego, CA, May 1990, pp. 961–962.

[2]Wie, B., Liu, Q., and Byun, K.-W., "Robust H_∞ Control Synthesis Method and its Application to a Benchmark Problem," American Control Conference, San Diego, CA, May 1990.

[3]Byun, K.-W., Wie, B., and Sunkel, J., "Robust Control Synthesis for Uncertain Dynamical Systems," *Proceedings of the AIAA Guidance, Navigation and Control Conference* (Boston, MA), AIAA, Washington, D.C., 1989 (AIAA Paper 89-3516).

[4]Byun, K.-W., Wie, B., Geller, D., and Sunkel, J., "Robust H_∞ Control Design for the Space Station with Structured Parameter Uncertainty," *Proceedings of the AIAA Guidance, Navigation and Control Conference* (Portland, OR), AIAA, Washington, DC, 1990 (AIAA Paper 90-3319).

[5]Byrns, E. V., Jr., and Calise, A. J., "Approximate Recovery of H_∞ Loop Shapes Using Fixed Order Dynamic Compensation," *Proceedings of the AIAA Guidance, Navigation and Control Conference* (New Orleans, LA), AIAA, Washington, DC, 1991 (AIAA Paper 91-2729).

[6]Kramer, F. S., and Calise, A. J., "Fixed Order Dynamic Compensation for Multivariable Linear Systems," *Journal of Guidance, Control, and Dynamics*, Vol. 11, No. 1, 1988, pp. 80–85.

[7]Tahk, M., and Speyer, J. L., "Modeling of Parameter Variations and Asymptotic LQG Synthesis," *IEEE Transactions on Automatic Control*, Vol. AC-32, No. 9, Sept. 1987, pp. 793–801.

[8]Doyle, J. C., Glover, K., Khargonekar, P. P., and Francis, B. A., "State Space Solutions to Standard H_2 and H_∞ Control Problems," *IEEE Transactions on Automatic Control*, Vol. AC-34, No. 8, 1989, pp. 831–847.

[9]Mendel, J. M., "A Concise Derivation of Optimal Constant Limited State Feedback Gains," *IEEE Transactions on Automatic Control*, Vol. AC-19, No. 4, Aug. 1974, pp. 447–448.

[10]Moerder, D. D., and Calise, A. J., "Convergence of a Numerical Algorithm for Calculating Optimal Output Feedback Gains," *IEEE Transactions on Automatic Control*, Vol. AC-30, Sept. 1985.

[11]Byrns, E. V., Jr., and Calise, A. J., "Fixed Order Dynamic Compensation for the H_2/H_∞ Benchmark Problem," *Proceedings of the American Control Conference*, San Diego, CA, May 1990, pp. 963–965.

[12]Wie, B., and Byun, K.-W., "New Generalized Structural Filtering Concept for Active Vibration Control," *Journal of Guidance, Control, and Dynamics*, Vol. 12, No. 2, 1989, pp. 147–154.

[13]Doyle, J. C., and Stein, G., "Multivariable Feedback Design: Concepts For a Classical/Modern Synthesis," *IEEE Transactions on Automatic Control*, Vol. AC-26, No. 1, 1981, pp. 4–10.